

Published in final edited form as:

Nat Chem Biol. 2012 November ; 8(11): 933–940. doi:10.1038/nchembio.1086.

An enzyme-trap approach allows isolation of intermediates in cobalamin biosynthesis

Evelyne Deery¹, Susanne Schroeder^{1,*}, Andrew D. Lawrence^{1,*}, Samantha L. Taylor¹, Arefeh Seyedarabi², Jitka Waterman³, Keith S. Wilson³, David Brown¹, Michael A. Geeves¹, Mark J. Howard¹, Richard W. Pickersgill², and Martin J. Warren¹

¹School of Biosciences, University of Kent, Canterbury, Kent, CT2 7NJ, UK.

²School of Biological and Chemical Sciences, Queen Mary University of London, Mile End Road, London E1 4NS, UK.

³Structural Biology Laboratory, Department of Chemistry, University of York, Heslington, York YO10 5DD, UK.

Abstract

The biosynthesis of many vitamins and coenzymes has often proved difficult to elucidate due to a combination of low abundance and kinetic lability of the pathway intermediates. Through a serial reconstruction of the cobalamin (vitamin B₁₂) pathway in *E. coli*, and by His-tagging the terminal enzyme in the reaction sequence, we have observed that many unstable intermediates can be isolated as tightly-bound enzyme-product complexes. Together, these approaches have been used to extract intermediates between precorrin-4 and hydrogenobyric acid in their free acid form and permitted the delineation of the overall reaction catalysed by CobL, including the formal elucidation of precorrin-7 as a metabolite. Furthermore, a substrate-carrier protein, CobE, has been identified, which can also be used to stabilize some of the transient metabolic intermediates and enhance their onward transformation. The tight association of pathway intermediates with enzymes provides evidence for a form of metabolite channeling.

Introduction

The isolation and characterization of biochemical pathways for vitamins and coenzymes has often proved technically challenging, mainly due to the low abundance and kinetic lability of the metabolic intermediates¹. Such is the case with the intermediates generated en route to the biosynthesis of adenosylcobalamin (vitamin B₁₂) (Fig. 1), the antipernicious factor. This biosynthesis requires around thirty enzyme-mediated steps for the complete *de novo* construction of the coenzyme and represents one of the most intricate syntheses found in nature^{2,3}. The biosynthesis of the corrin-ring component is mediated via distinct aerobic and anaerobic pathways that oversee the transformation of the tetrapyrrole primogenitor, uroporphyrinogen III, into cobyrinic acid.

Correspondence to: M. J. Warren, tel 00 44 (0)1227 824690, m.j.warren@kent.ac.uk or R. W. Pickersgill, tel 00 44 (0)20 7882 8444, r.w.pickersgill@qmul.ac.uk.

*Made an equal contribution to the work

Author contributions ED designed and performed most of the experiments and analysis with support of ADL and SS; ADL performed mass spectroscopy analysis. SLT performed all NMR data acquisition, which was analysed with MJH. SS, AS and RWP contributed the CobL^C and CobH-HBA structures and CobL and CobE-HBA models. JV and KSW contributed the CobE structure. DB and SS determined the CobH-5-desmethyl HBA structure. MAG provided insight into substrate channeling. MJW directed all aspects of the project. ED and MJW wrote the manuscript.

Competing Financial Interests Statement. The authors have no competing financial interest.

Corrin ring synthesis involves significant decoration of the tetrapyrrole framework and includes the chemically challenging process of ring contraction to expel the C20 *meso* position to allow for the tighter coordination of the centrally chelated cobalt ion²⁻⁴. Overall, the transformation of uroporphyrinogen III into hydrogenobyric acid (HBA), the first stable intermediate along the pathway^{5,6}, involves 8 *S*-adenosyl-*L*-methionine (SAM) - dependent methylations, extrusion of an integral macrocyclic carbon atom (ring contraction), decarboxylation of an acetate side chain and methyl migration³ (Fig. 1). There are a number of specific questions still to be addressed on the mechanisms underpinning many of these transformations as well as general questions about how pathways handle large numbers of labile intermediates and how such intricate pathways evolved.

This paper addresses some of these questions through a study of the aerobic cobalamin pathway, which is outlined in Fig.1. The intermediates of the pathway are termed precorrin-*n*, where *n* refers to the number of methyl groups that have been added to the framework⁷. The pathway is initiated by the action of a *bis*-methylase, CobA, which methylates uroporphyrinogen III at positions 2 and 7 to generate precorrin-2⁸. A further methylation at C20 by CobI synthesizes precorrin-3A⁹. This acts as the substrate for the monooxygenase CobG, which generates a tertiary alcohol at C20 and forms a γ -lactone with the acetate side chain on ring A^{10,11} (precorrin-3B). Another methyltransferase, CobJ, methylates at C17 and mediates ring contraction by catalyzing a masked pinacol rearrangement^{11,12}. Additional methylations by CobM and CobF at C11 and C1, the latter with loss of the extruded C20 position as acetic acid, results in the synthesis of precorrin-5 and precorrin-6A, respectively^{13,14}. The macrocyclic ring system is reduced by the action of CobK, producing precorrin-6B¹⁵. This is the substrate for CobL, a multifunctional enzyme, that promotes the decarboxylation of the acetic acid side chain at C12 and methylation at the northern (C5) and southern (C15) *meso* positions and in so doing makes precorrin-8¹⁶. Finally, CobH catalyzes a 1,5-sigmatropic rearrangement that sees the migration of the methyl group from C11 to C12, generating HBA¹⁷.

Most of the aforementioned intermediates have only been isolated after esterification and in very small quantities. Yet to investigate further many of these highly unusual reactions simple reproducible protocols need to be established for the production of these compounds. To achieve this we attempted building the pathway recombinantly in *E. coli*, an organism that does not house the cobalamin biosynthetic pathway. We demonstrated that it was possible to generate HBA in *E. coli*⁶ by overproducing enzymes (CobA-I-G-J-M-F-K-L-H) that manage the transformation of uroporphyrinogen III into the comparatively stable orange-colored HBA. This ring-contracted corrin intermediate can be purified from a cell lysate of this strain by ion exchange and reverse phase chromatography⁶. However, attempts to produce the intervening intermediates between uroporphyrinogen III and HBA using the same strategy of building the pathway one enzyme at a time were not successful. It appears that the intermediates are too unstable to be purified.

In this paper we outline a strategy for the isolation of five pathway intermediates between precorrin-4 and HBA in their free acid forms, stabilized as protein complexes. This approach resulted in the isolation and characterization of a new intermediate along the pathway, precorrin-7 (1), the use of this template for the combinatorial synthesis of a new pathway analogue and the identification of pathway carrier protein. The results have implications not only for understanding how complex pathways enhance and control the stability of labile intermediates by substrate channeling but also for how pathways can be manipulated for the synthesis of cofactor analogues.

Results

Enzymes as traps for pathway intermediates

In the absence of a downstream enzyme in a pathway we wondered if labile intermediates could be stabilized as enzyme-product complexes. To investigate this we constructed a number of plasmids where the corrin pathway was built up in an ordered fashion but where the terminally-encoded enzyme also contained a His-tag. In this way it should be possible to isolate quickly the terminal enzyme in the pathway and determine if it contains any bound intermediate. Thus, the following constructs were made: *cobA-I-G-J**, *cobA-I-G-J-M**, *cobA-I-G-J-M-F**, *cobA-I-G-J-M-F-K**, *cobA-I-G-J-M-F-K-L** and *cobA-I-G-J-M-F-K-L-H** (where the asterisk represents a His-tagged encoded version of the gene).

After *E. coli* was transformed with these plasmids and the His-tagged protein purified from the appropriate individual strains it was found that CobJ*, CobM*, CobF*, CobK* and CobH* all purified with an associated chromophore that varied in color from blue to yellow and red (Fig. 2). Only CobL* failed to purify with a bound pigment. An SDS gel of the isolated His-tagged proteins is shown in Supplementary Results, Supplemental Fig. 1.

Isolation of precorrin-4 and factor IV with CobJ*

When CobJ* was isolated aerobically from the recombinant strain harboring *cobA-I-G-J**, the protein purified with a strong blue coloration. The spectrum obtained from this blue pigment-protein complex had maxima at 378, 477, 510, 593, and 641 nm (Fig. 2a) whilst the free pigment had a mass of m/z 907 (M^+H), all of which is consistent with the presence of factor IV¹², the oxidized form of precorrin-4.

When the purification was repeated under anaerobic conditions CobJ* was found to purify with a yellow color, consistent with the presence of precorrin-4 (Fig. 2a). Exposure of the anaerobically isolated CobJ to oxygen led to a rapid transformation into the blue pigment. Evidence that the yellow pigment was precorrin-4 came from incubating this protein-bound complex with SAM, NADPH and purified CobF, CobM, CobK, CobL and CobH, which resulted in the appearance of the orange-colored HBA and its characteristic spectrum (data not shown).

Isolation of complexes with CobF* and CobM*

A very light yellow pigment was isolated with CobM* after extraction and purification of the protein by immobilized metal affinity chromatography from the recombinant strain harboring *cobA-I-G-J-M** (Fig. 2b) while a dark yellow pigment was observed associated with CobF* after its purification from the strain containing *cobA-I-G-J-M-F** (Fig. 2c). The spectra obtained from CobM* and CobF* were not very defined and the attached chromophores were not characterized in detail. Moreover, incubation of these complexes with the downstream enzymes for HBA synthesis did not result in the production of HBA. Thus the compounds bound to CobM* and CobF* are not pathway intermediates and are likely to represent either oxidized products or derailed pathway analogues. Such derailed analogues have been observed previously and result from either overmethylation or mis-methylation^{18,19}, a consequence of a particularly high concentration of biosynthetic enzyme.

Isolation of precorrin-5 and -6A

Although precorrin-5 and -6A were not found associated with CobM* and CobF* these intermediates could be generated by adding the enzymes sequentially to the CobJ-precorrin-4-complex. Thus, addition of SAM and CobM resulted in the appearance of precorrin-5 (Fig. 2b), a pale yellow compound that was very unstable and which turned purple within minutes inside the anaerobic chamber in the absence of the next enzyme of the

pathway. This purple material appears to be a dead-end compound as addition of further enzymes did not result in any further spectral changes. Addition of SAM plus CobM and CobF to the CobJ-precorrin-4-complex generated precorrin-6A (Fig. 2c). This could be rapidly reduced to precorrin-6B when it was incubated with NADPH and CobK, while the further addition of CobL lead to the appearance of precorrin-8, from which HBA was produced by the addition of CobH (data not shown).

Isolation of precorrin-6B

When CobK* was produced and purified from the recombinant strain containing *cobA-I-G-J-M-F-K**, it was found associated with a yellow pigment that had an absorption maximum at 348 nm (Fig. 2d). This enzyme-product complex could be converted into HBA by incubation with the downstream enzymes CobL and CobH (data not shown). When released from CobK the intermediate was found to have a mass of 897.4 (M⁺H), which is that expected for precorrin-6B.

CobL* does not form a stable enzyme-product complex

The only protein within this section of the cobalamin biosynthetic pathway that does not appear to bind anything substantial is CobL. Thus, CobL* isolated from the strain harboring *cobA-I-G-J-M-F-K-L** gave a very bland spectrum with only minor absorbances (Fig. 2e, f).

CobH* binds HBA

When CobH* was purified from the strain harboring *cobA-I-G-J-M-F-K-L-H** it was found to purify with a strong orange chromophore (Fig. 2g and Supplemental Fig. 2). A UV-visible scan of the protein solution showed that it contained a slightly altered UV-visible spectrum of HBA, with absorption maxima at 330 and 484 nm (Fig. 2g). The CobH*-HBA complex could be dissociated by boiling, which resulted in a concomitant change in the spectrum to that of free HBA with absorption maxima at 329, 496 and 522 nm (Fig. 2g) and a mass of m/z 881.4 (M⁺H) was observed by mass spectroscopy. The structure of this free acid form of HBA was further confirmed by NMR (Supplemental Table 1a) and by the crystallization (Supplemental Fig. 2) and subsequent X-ray structure determination of the CobH-HBA complex. Previous reports have highlighted a tight association between CobH and HBA^{17,20}.

CobE binds a number of different intermediates

The lack of a binding protein for precorrin-8 led us to think that this role could be played by CobE, whose function within the aerobic B₁₂ pathway has been the subject of some speculation⁴. In the current work we have shown that CobE is not required for the *in vitro* transformation of precorrin-4 into HBA as this conversion is mediated by CobM, F, K, L and H alone. To investigate the possibility that CobE may act as a substrate carrier *cobE* was modified in such a manner so as to include a fusion encoding a hexahistidine tag (CobE*) and then cloned in tandem into a range of plasmids with the genes responsible for the production of precorrin-4, precorrin-5, precorrin-6A, precorrin-6B, precorrin-8 or HBA. This resulted in the following constructs: *cobA-I-G-J-E**, *cobA-I-G-J-M-E**, *cobA-I-G-J-M-F-E**, *cobA-I-G-J-M-F-K-E**, *cobA-I-G-J-M-F-K-L-E** and *cobA-I-G-J-M-F-K-L-H-E**. Encouragingly, when CobE* was isolated from the resulting strains transformed with these plasmids the protein was found to purify associated with a range of different pigments (Fig. 2). An SDS gel of CobE* isolated from these strain is shown in Supplemental Fig. 1.

When CobE* was isolated from the strain harboring *cobA-I-G-J-E** there was little evidence of anything binding to the protein (Fig. 2a). However, when CobE* was isolated from strains with the genes required for precorrin-5 and precorrin-6A (i.e. from strains containing

*cobA-I-G-J-M-E** and *cobA-I-G-J-M-F-E** respectively) the protein was found to purify with strong absorption spectra (Fig. 2b, c). The spectra did not correspond to free precorrin-5 or precorrin-6A but did have some similarity to the spectra observed with CobM* and CobF*. Unfortunately, as with CobM* and CobF*, incubation of the isolated CobE*s from the precorrin-5 and precorrin-6A strains with the downstream enzymes for HBA synthesis did not result in a change in the spectra. More encouragingly, CobE* isolated from the strain with the genetic components for precorrin-6B synthesis (i.e. containing *cobA-I-G-J-M-F-K-E**) had a broad absorption spectrum around 350 nm, although it is not as defined as the product-complex spectrum that was observed when CobK* was purified (Fig. 2d). Significantly, incubation of this CobE* protein with CobL and CobH resulted in the production of HBA. Thus CobE* has the ability to bind precorrin-6B.

CobE* was also found to bind precorrin-8 and HBA since isolation of CobE* from strains harboring *cobA-I-G-J-M-F-K-L-E** and *cobA-I-G-J-M-F-K-L-H-E** resulted in yellow and orange colored protein, respectively (Fig. 2f, g). The yellow color was shown to be precorrin-8 as incubation of this protein with CobH resulted in HBA production. The structure of precorrin-8 was confirmed by NMR (Supplemental Table 1b). It is interesting to note that CobE is able to bind precorrin-8 whereas CobL does not. Overall, therefore, CobE is able to bind precorrin-6B, precorrin-8 and HBA. As a result, we propose that its role in the aerobic pathway is to act as a substrate carrier protein or substrate chaperone, binding excess labile compounds and ensuring that they are delivered to the next enzyme in the pathway.

To support this theory we observed that CobE was able to stabilize precorrin-8. When left free in solution precorrin-8 bleaches with a half-life of 3-4 hours (Fig. 3a and Supplemental Fig. 3). In contrast, when bound to CobE, comparatively little precorrin-8 is lost (Fig. 3a). Moreover, the yield of HBA from precorrin-6B through incubation with CobL, CobH and SAM, is approximately doubled in the presence of CobE (Fig 3b and Supplemental Fig. 3). In order to understand how CobE, which is a comparatively small protein of around 150 amino acids, may act to stabilize the various pathway intermediates that it binds, the structure of the protein was solved by X-ray crystallography (Fig. 3c). This revealed that CobE has a globular α/β fold with dimensions approximately $30 \times 35 \times 35 \text{ \AA}^3$, with a single domain containing a five-stranded β -sheet with five associated α -helices and one 3_{10} -helix (Fig. 3c). The β -sheet and α -helices α_5 and α_6 create the walls of a cleft of approximate dimensions $8 \times 15 \times 17 \text{ \AA}^3$. The cleft is likely to be the binding site of the protein and in the present structure several non-protein ligand molecules are bound therein. The presence of conserved basic residues lining this cleft strongly suggests their involvement in binding groups, such as the negative charges on the side chain groups of the corrin ring. Modeling of HBA in the cavity suggests that CobE can easily accommodate molecules the size of HBA in a slightly bent conformation both in terms of shape and electrostatic complementarity (Fig. 3d), though further experimental evidence is needed to confirm the scope of CobE function.

Although crystallography of CobE-bound complexes has not yet been achieved, NMR spectra of CobE bound to a range of compounds were recorded. ^{15}N , ^1H HSQC spectra of CobE before and after the addition of HBA and precorrin-6B (Supplemental Fig. 4a-b) support binding of the intermediates by this protein. Changes in chemical shifts further suggest that a significant structural change in CobE must occur upon interaction. Closer inspection of the data (Supplemental Fig. 4) confirm both similarities and differences between the chemical shift changes observed for CobE with each intermediate. Apo CobE ^{15}N HSQC data contains 62% of the resonances expected for the protein with this number rising to 80% in the presence of ligands. To probe the specificity of binding of HBA to CobE further, quenching fluorescence assays were performed that confirmed a 1:1

stoichiometric HBA-CobE interaction with a $K_d = 0.08 \mu\text{M}$ (Supplemental Fig. 5). Additionally, ^{15}N HSQC NMR titration curve datasets were created using variable final concentrations between 0.0 and 1.0 mM of HBA with a final constant 0.2 mM concentration of CobE. Tracking of HBA addition using chemical shift changes confirmed the tight interaction observed by fluorescence quenching ($K_d = 0.12 \mu\text{M}$; Supplemental Fig. 6a). Fitting this data also yielded a second event with a lower K_d of $309 \mu\text{M}$ (Supplemental Fig. 6b), though the basis for this is unknown.

CobL dissection

With the basis for CobE function established, we returned to the one enzyme that had proven uninformative in the reconstruction assays, CobL. The precorrin-6B/CobK* complex was used to study the reaction catalyzed by CobL, which is responsible for the C5 and C15 methylations and the decarboxylation of the acetate side chain attached to the C12. When precorrin-6B-bound CobK was incubated with SAM and CobL, the solution turned a brighter yellow shade associated with the generation of precorrin-8 (Supplemental Fig. 7). Analysis of the resulting compound revealed that it had a mass of m/z of 881.4 (M^+H) in agreement with such a transformation.

Comparative studies suggest that CobL has arisen from a fusion between two separate classes of SAM methyltransferases, the canonical B_{12} -biosynthetic class III type and a class I methyltransferase. Indeed, in the anaerobic pathway the orthologue of CobL is sometimes found as two separate genes, which is the case in *Salmonella enterica* where they are termed CbiE and CbiT. In order to investigate the role played by the two regions within CobL the gene was dissected to give *cobL^N*, which encodes the N-terminal part of CobL, and *cobL^C*, which encodes the C-terminal domain of CobL (Fig. 4a, and Supplemental Fig. 8 for sequence alignment). The two fragmented genes were cloned individually into pET14b and transformed into *E. coli* BL21 cells to allow the production of their encoded dissected protein products. Incubation of the precorrin-6B/CobK* complex with CobL^N and SAM did not alter the original spectrum (Supplemental Fig. 7) whereas, in contrast, the same incubation with CobL^C and SAM resulted in the appearance of a yellow pigment with a spectrum that was slightly shifted in comparison to that of precorrin-8 (Supplemental Fig. 7). Mass spectral analysis of this compound was consistent with the decarboxylation and monomethylation of precorrin-6B, precorrin-7 (m/z of 867.4 (M^+H)). This is the first time this compound had been isolated. Precorrin-7 could subsequently be transformed into precorrin-8 by the addition of full length CobL, but not CobL^N (Supplemental Fig. 7). It would thus appear that CobL^N was inactivated by the dissection procedure.

An insight into the structure/function of CobL was initiated via X-ray crystallography. Although CobL did crystallize the diffraction was poor and reliable protein phases have yet to be determined. However, CobL^C also crystallized and this structure was determined to 2.7 Å resolution (Fig. 4b). The SAH and putative precorrin binding sites are away from the subunit interface and open to solvent. The SAH binding site is at the C-terminal end of β -strands 1, 2, and 3, sandwiched between two glycine rich loops and adjacent to the putative precorrin-6B binding cleft (Fig. 4c). The structure of CobL can now be modeled using the solved structure of the C-terminal domain, which forms a tetramer, plus two dimers of the closest canonical methyltransferase, *Archaeoglobus fulgidus* CbiE (Supplemental Fig. 9). Each of the four protein chains in the tetramer has two SAH binding sites, one in the C-terminal non-canonical and one in the N-terminal canonical domain. The tetramer is a dimer of dimers with the active centers apparently independent in this model. The active sites are not juxtaposed, so there is apparently no simple transfer of precorrin-7 from the active centre of the C-terminal domain to the N-terminal domain. However, this role could be played by CobE, and such a model would predict that CobE would also bind precorrin-7. The positioning of the C-terminal domain relative to the N-terminal domain of CobL, while not

bringing the active centers of the two domains close together, could influence the accessibility of the N-terminal domain's active centre to CobE or CobH.

Isolation and characterization of precorrin-7

To investigate the ability of CobE to bind precorrin-7, CobE* was produced in a strain harboring *cobA-I-G-J-M-F-K-L^C-E**. The protein was, indeed, found to purify with precorrin-7 attached (Fig. 2e). As with precorrin-8, CobE also appears to stabilize precorrin-7 since the bound complex has an extended half life in comparison to the unbound intermediate, where the binding can also be monitored by NMR (Supplemental Fig. 4c). After the protein was gently denatured NMR analysis of the liberated precorrin-7 was undertaken. The data support the presence of major and minor tautomeric states (Supplemental Table 1c) that differ in the presence of a proton attached at the C8 position in the minor state (Supplemental Fig. 10). This was confirmed from ¹³C-¹H HSQC (Heteronuclear Single Quantum Correlation spectroscopy), HMBC (Heteronuclear Multiple Bond Correlation spectroscopy) and TOCSY (TOtal Correlation Spectroscopy) datasets (Supplemental Fig. 11). Such resonances are broad, suggesting strong evidence for chemical exchange in this state. ¹H-¹³C HSQC spectra were also collected at 5°C and 40°C in an attempt to minimize the presence of the minor form but further deconvolution of the data was not possible.

The major state of precorrin-7 is consistent with the data shown in Supplemental Table 1c. The NMR confirms the presence of methyl groups at positions C1, C2, C7, C11, C12, C15 and C17. This demonstrates that CobL^C is responsible for the C15 methylation and decarboxylation of the acetate side chain on C12. From a mechanistic perspective it is likely that the decarboxylation and methylation are concerted reactions (Fig. 5).

To generate a form of CobL that only has C5 methylase activity, with no C15 methylase/ decarboxylase activity, two separate point mutations, G257R and E276A, were introduced in the SAM binding site of the CobL^C domain of full-length CobL (Fig. 4c and Supplemental Fig. 8). Incubation of CobL^{G257R} or CobL^{E276A} with precorrin-6B-bound CobK and SAM did not alter the spectrum of the substrate. However, when CobL^C was added to the reaction, the spectrum of precorrin-8 was produced (Supplemental Fig. 7), which changed to HBA when CobH was added. CobL^{G257R} or CobL^{E276A} are therefore able to use precorrin-7 as a substrate and function solely as C5 methyltransferases (Supplemental Fig. 7). These series of experiments clearly delineate the reaction sequence for the transformation of precorrin-6B into precorrin-8.

Synthesis of C5-desmethyl-HBA

A further surprising result was obtained by incubating precorrin-7 with CobH. Here the compound with an absorption maximum at 397 nm was readily transformed into a compound with a spectrum that was similar to, but distinct from, HBA (Supplemental Fig. 12). Mass spectral analysis of this new compound revealed that it is 14 mass units smaller than HBA, consistent with the formation of C5-desmethyl-HBA (2) (m/z of 867.4 (M⁺H)). It would thus appear that precorrin-7 acts as an out-of-turn substrate for CobH. The structure of the compound was confirmed by crystallizing the CobH-desmethyl-HBA complex, from which the resulting 1.4 Å data clearly revealed the absence of the C-5 methyl group (Fig. 5).

Discussion

This report describes an approach for trapping intermediates involved in the cobalamin biosynthetic pathway in their natural (free acid) form as enzyme-product complexes. CobJ, CobK and CobH, were found to bind their products tightly and protect them from the

external environment. Furthermore, CobE, a protein to which no function had been formally assigned, was found to associate with a number of intermediates including precorrin-6B, precorrin-7, precorrin-8 and HBA. Our *in vitro* data supports a role for CobE in the stabilization of intermediates such as precorrin-7 and precorrin-8, most likely through binding to the large crevice found at the opposite end of the protein to the N and C termini. The inclusion of CobE in *ex vivo* assays of precorrin-6B to HBA also leads to an enhancement in overall yield. Thus, CobE plays a role as a substrate carrier or chaperone protein, shuttling labile intermediates between different Cob enzymes.

The observation that several stable enzyme-product complexes can be isolated from the aerobic pathway is unusual for a metabolic pathway and is probably linked to the low stability of the pathway intermediates. The high affinity of the intermediates for the enzymes require very low dissociation rate constants that are incompatible with the expected flux through the pathway. This implies that the enzymes retain the unstable intermediates until some signal or interaction allows the release of the product to be efficiently used by the next enzyme in the pathway. The established hypothesis for such behaviour is called *metabolite channelling* – that is the enzyme holds onto its product to pass it efficiently if not directly onto the succeeding step in the biosynthesis. At one time this was a contentious area^{21,22} but there are now several clear-cut examples where substrate channelling does occur (for reviews see²³⁻²⁵). We believe that this is the first report of a series of enzymes that form stable product complexes, in the absence of a stable multienzyme complex. Channelling requires a series of transient interactions between the enzymes along the pathway to allow intermediates to be passed from enzyme to enzyme. Given that the cytoplasm of *E. coli* appears as a sieve that permits the diffusion of small molecules while limiting the movement of larger ones^{26,27} the observed formation of stable enzyme-product complexes would suggest that the enzymes of the cobalamin pathway must loosely associate in the form of a metabolon²⁸ to allow the pathway to operate.

However, our research does not differentiate between “real channelling” and “enhanced transfer” between enzymes, which can occur between two enzymes if there is a higher probability of substrate rebinding to the downstream enzyme. This will require further research to measure the loss of substrate to side reactions as a function of enzyme concentration in pairs of enzymes and in the complete pathway.

The research describes a simple but highly efficient method for the isolation of pathway intermediates, thereby allowing the elucidation of metabolic pathways in a fairly rapid timescale. This method will be particularly applicable to pathways involving labile compounds. This report also describes the combinatorial synthesis of a non-physiological corrin analogue, 5-desmethyl-HBA. Such an approach could be used to make a range of cobalttoporphyrin and corrin derivatives, molecules that are of increasing interest in the bioenergy field since they have been shown to have the ability to oxidize water^{29,30}. It can also be used to make useful probes for the study of cobalamin-dependent reactions and derivatives of the cofactor for enhanced drug delivery³¹.

Methods

Construction of plasmids

All cobalamin biosynthetic genes were amplified by PCR using genomic DNA from either *Rhodobacter capsulatus* SB1003 (*cobA, I, J, F, M, K, L and H*), *Brucella melitensis* 16M (*cobG, cobE*), *Pseudomonas denitrificans* (*cobG*) (gift from Dr C. Roessner, Texas A & M University) or *Pseudomonas aeruginosa* (*cobE*). The *cob* genes were amplified individually with primers containing either *AseI* or *NdeI* restriction sites at the 5' end and a *SpeI* site at the 3' end to allow them to be cloned contiguously within the plasmid as previously

described⁶. Genes were cloned into modified pET3a and pET14b plasmids as highlighted in Supplementary Table 2.

Recombinant protein overproduction and purification

E. coli strain BL21 star (DE3) pLysS was transformed with the relevant plasmids. The recombinant strains were grown in LB at 37°C. The protein overproduction was induced with isopropyl 1-thio-β-D-galactopyranoside (0.4 mM). The cells were resuspended in buffer A (500 mM NaCl, 5 mM imidazole, 20 mM HEPES, pH 7.5) and sonicated. The protein was purified using Chelating SepharoseTM charged with NiSO₄. Unbound proteins were washed off with buffer A and with buffer A containing 60 mM imidazole. Proteins were eluted with buffer A containing 400 mM imidazole and passed through a PD10 column equilibrated with buffer B (20 mM HEPES pH 7.5 and 100 mM NaCl).

Purification of proteins with trapped intermediates

The different *E. coli* strains transformed with a plasmid encoding multiple proteins of which a unique histidine-tagged protein binding the trapped intermediate were grown in 2YT at 28°C for 24 hours. The protein purification procedure was identical to the method above except that NaCl was lowered to 100 mM.

Site-directed mutagenesis

The CobL G257R mutant was created using the QuickChange II site-directed mutagenesis (Agilent). The CobL E276A was constructed following the site-specific mutagenesis by overlap extension protocol³².

Assays from PC4 to HBA or C5-desmethyl-HBA

All assays were performed in buffer B. SAM was added at a final concentration of 0.58 mM, NADPH at 15 μM and all proteins were added at 2 μM. The reactions were incubated at room temperature. Anaerobic conditions were obtained using an anaerobic glove-box (Belle Technology).

Mass spectrometry

Samples were separated on an Agilent 1100 series HPLC coupled to a micrOTOF-Q II (Bruker) mass spectrophotometer using an Ace 5 AQ column (2.1 × 150 mm; Advanced Chromatography Technologies) maintained at 30°C and with a flow rate of 0.2 ml/min. The mobile phase consisted of 0.1% acetic acid (v/v) in water (solvent A) and 100% methanol (solvent B). The initial conditions were set at 95% A, 5% B. The concentration of solvent B was increased with a linear gradient to 80% over 30 min and back to the initial conditions at 40 min. The mass spectrometer was operated in the positive electrospray mode.

NMR of precorrin-7, precorrin-8 and HBA

Samples of precorrin-7, precorrin-8 and HBA for NMR analysis were prepared from their respective strains bound to either CobE* or CobH*. Precorrin-7 and precorrin-8 were purified trapped with CobE as described above whereas HBA was trapped with CobH. The complexes were then heated to denature the protein and leave the intermediate free in solution. After lowering the pH to around 5, the pigments were applied to LiChroprep RP18 columns. The compounds were briefly washed with water and eluted in 50% ethanol. After lyophilization, they were finally dissolved in deuterium oxide (99.9% atom D). All NMR experiments were carried out using a 600 MHz (¹H) Varian UnityINOVA spectrometer a 5 mm z-PFG HCN NMR probe or a 600 MHz (¹H) Bruker Avance III spectrometer with a 5 mm QCI-F cryoprobe.

NMR details are given in the supplementary information. ^1H Chemical shift referencing was based on the position of the water resonance, ^{13}C referencing used $^1\text{H}/^{13}\text{C}$ gyromagnetic ratios to define indirect carrier position³³ and all data were obtained at 25°C unless otherwise stated. Data processing was completed using NMRPipe³⁴ and resonance assignments were completed using CCPN analysis 2³⁵.

Crystallography

CobE crystals were obtained from 0.1M MES buffer pH 6.9, 2 M ammonium sulphate and 5% dioxane³⁶ and the structure solved as outlined in the Supplemental information. The final R-factor and R-free are 0.194 and 0.268 respectively for a model with good stereochemistry (Supplemental Table 3a). CobL^C crystals were produced as described previously³⁷ and solved at 2.7 Å by molecular replacement using the *C. diphtheriae* putative precorrin-6Y C5,15-methyltransferase targeted domain structure (PDB code: 3hm2) as a search model. The *C. diphtheriae* methyltransferase sequence is 41 % identical to that of *R. capsulatus* CobL^C and MOLREP³⁸ gave a model with a score of 0.314 that could be successfully rebuilt and refined using CNS³⁹ and BUCANEER⁴⁰/REFMAC⁴¹ with manual rebuilding using COOT⁴² (Supplemental Fig. 9). The final R-factor and R-free are 0.185 and 0.254 respectively for a model with good stereochemistry (Supplemental Table 3b). The CobH complexes were crystallized using 25-30% PEG 8K, 0.2 M ammonium sulfate and 0.1 M cacodylate pH 6.5. The structures were solved by molecular replacement using 111H²⁰ and refined using similar methods to those described for CobL^C (Supplemental Table 3c)⁴³⁻⁴⁵. Coordinates and structure factor amplitudes have been deposited in the protein databank with accession codes: 2BSN (CobE), 3NJR (CobL^C), 4FDV (CobH-HBA) and 4AU1 (CobH-desmethyl-HBA).

Molecular modeling

Docking was used to fit HBA into the binding cavity of CobE. There was a single orientation of HBA that fitted well with the acidic side chains mapping to basic regions of CobE. No adjustments of the conformation of HBA or CobE were necessary. The CobL structure was modeled by docking the N-terminal domains of CbiE onto the C-terminal domains of CobL^C. Again this was a straightforward modeling procedure achieved using molecular docking in PyMOL.

Supplementary Material

Refer to Web version on PubMed Central for supplementary material.

Acknowledgments

This work was supported by grants from the Biotechnology and Biological Sciences Research Council (BBSRC) BB/E024203 and BB/I013334 and the Wellcome Trust 091163/Z/10/Z. We thank Dr. Michelle Rowe for additional NMR technical support. Diffraction data were collected at the European Synchrotron Radiation Facility, Grenoble, France (for CobE) and the Diamond Light Source, Oxfordshire, UK (for CobL & CobH).

References

1. Webb ME, Marquet A, Mendel RR, Rebeille F, Smith AG. Elucidating biosynthetic pathways for vitamins and cofactors. *Nat. Prod. Rep.* 2007; 24:988–1008. [PubMed: 17898894]
2. Battersby AR. How nature builds the pigments of life: the conquest of vitamin B12. *Science.* 1994; 264:1551–1557. [PubMed: 8202709]
3. Warren MJ, Raux E, Schubert HL, Escalante-Semerena JC. The biosynthesis of adenosylcobalamin (vitamin B12). *Nat. Prod. Rep.* 2002; 19:390–412. [PubMed: 12195810]

4. Blanche F, et al. Vitamin B12: How the problem of its biosynthesis was solved. *Angew. Chem. Int. Ed. Engl.* 1995; 34:383–411.
5. Blanche F, et al. Hydrogenobyric Acid - Isolation, Biosynthesis, and Function. *Angew. Chem. Int. Edit.* 1990; 29:884–886.
6. McGoldrick HM, et al. Identification and characterization of a novel vitamin B12 (cobalamin) biosynthetic enzyme (CobZ) from *Rhodobacter capsulatus*, containing flavin, heme, and Fe-S cofactors. *J. Biol. Chem.* 2005; 280:1086–1094. [PubMed: 15525640]
7. Uzar HC, Battersby AR, Carpenter TA, Leeper FJ. Biosynthesis of Porphyrins and Related Macrocycles .28. Development of a Pulse Labeling Method to Determine the C-Methylation Sequence for Vitamin-B12. *J. Chem. Soc. Perk. T.* 1987; 1:1689–1696.
8. Blanche F, Debussche L, Thibaut D, Crouzet J, Cameron B. Purification and characterization of S-adenosyl-L-methionine: uroporphyrinogen III methyltransferase from *Pseudomonas denitrificans*. *J. Bacteriol.* 1989; 171:4222–4231. [PubMed: 2546914]
9. Warren MJ, et al. Enzymatic synthesis and structure of precorrin-3, a trimethyldipyrrocorphin intermediate in vitamin B12 biosynthesis. *Biochemistry.* 1992; 31:603–609. [PubMed: 1731915]
10. Debussche L, et al. Biosynthesis of vitamin B12: Structure of precorrin-3B, the trimethylated substrate of the enzyme catalysing ring contraction. *J. Chem. Soc., Chem. Commun.* 1993:1100–1103.
11. Scott AI, et al. Biosynthesis of vitamin B12. Discovery of the enzymes for oxidative ring contraction and insertion of the fourth methyl group. *FEBS Letts.* 1993; 331:105–108. [PubMed: 8405386]
12. Thibaut D, Debussche L, Frechet D, Herman F, Vuilhorgne M, Blanche F. Biosynthesis of vitamin-B12 - the structure of factor-IV, the oxidized form of precorrin-4. *J. Chem. Soc., Chem. Commun.* 1993:513–515.
13. Min C, Atshaves BA, Roessner CA, Stolowich NJ, Spencer JB, Scott AI. Isolation, structure and genetically engineered synthesis of precorrin-5. *J. Am. Chem. Soc.* 1993; 115:10380–10381.
14. Thibaut D, Blanche F, Debussche L, Leeper FJ, Battersby AR. Biosynthesis of vitamin B12: structure of precorrin-6x octamethyl ester. *Proc. Nat.l Acad. Sci. USA.* 1990; 87:8800–8804.
15. Blanche F, et al. Precorrin-6x reductase from *Pseudomonas denitrificans*: purification and characterization of the enzyme and identification of the structural gene. *J. Bacteriol.* 1992; 174:1036–1042. [PubMed: 1732193]
16. Blanche F, et al. Biosynthesis of vitamin B12 in *Pseudomonas denitrificans*: the biosynthetic sequence from precorrin-6y to precorrin-8x is catalyzed by the cobL gene product. *J. Bacteriol.* 1992; 174:1050–1052. [PubMed: 1732195]
17. Thibaut D, et al. The final step in the biosynthesis of hydrogenobyric acid is catalyzed by the cobH gene product with precorrin-8x as the substrate. *J. Bacteriol.* 1992; 174:1043–1049. [PubMed: 1732194]
18. Santander PJ, Kajiwarara Y, Williams HJ, Scott AI. Structural characterization of novel cobalt corrinoids synthesized by enzymes of the vitamin B-12 anaerobic pathway. *Bioorg. Med. Chem.* 2006; 14:724–731. [PubMed: 16198574]
19. Scott AI, Warren MJ, Roessner CA, Stolowich NJ, Santander PJ. Development of an Overmethylation Strategy for Corrin Synthesis - Multienzyme Preparation of Pyrrocorphins. *J. Chem. Soc., Chem. Comm.* 1990:593–597.
20. Shipman LW, Li D, Roessner CA, Scott AI, Sacchettini JC. Crystal Structure of Precorrin-8x Methyl Mutase. *Structure with Folding & Design.* 2001; 9:587–596. [PubMed: 11470433]
21. Pettersson G. No Convincing Evidence Is Available for Metabolite Channeling between Enzymes Forming Dynamic Complexes. *J. Theor. Biol.* 1991; 152:65–69. [PubMed: 1753770]
22. Wu XM, Gutfreund H, Lakatos S, Chock PB. Substrate channeling in glycolysis: a phantom phenomenon. *Proc. Natl. Acad. Sci. USA.* 1991; 88:497–501. [PubMed: 1988948]
23. Huang XY, Holden HM, Raushel FM. Channeling of substrates and intermediates in enzyme-catalyzed reactions. *Ann. Rev. Biochem.* 2001; 70:149–180. [PubMed: 11395405]
24. Jorgensen K, et al. Metabolon formation and metabolic channeling in the biosynthesis of plant natural products. *Curr. Opin. Plant Biol.* 2005; 8:280–291. [PubMed: 15860425]

25. Miles EW, Rhee S, Davies DR. The molecular basis of substrate channeling. *J. Biol. Chem.* 1999; 274:12193–12196. [PubMed: 10212181]
26. McGuffee SR, Elcock AH. Diffusion, crowding & protein stability in a dynamic molecular model of the bacterial cytoplasm. *PLoS Comput. Biol.* 2010; 6:e1000694. [PubMed: 20221255]
27. Mika JT, van den Bogaart G, Veenhoff L, Krasnikov V, Poolman B. Molecular sieving properties of the cytoplasm of *Escherichia coli* and consequences of osmotic stress. *Mol. Micro.* 2010; 77:200–207.
28. Robinson JB Jr, Inman L, Sumegi B, Srere PA. Further characterization of the Krebs tricarboxylic acid cycle metabolon. *J. Biol. Chem.* 1987; 262:1786–1790. [PubMed: 2433288]
29. Dogutan DK, et al. Hangman corroles: efficient synthesis and oxygen reaction chemistry. *J. Am. Chem. Soc.* 2011; 133:131–140. [PubMed: 21142043]
30. Lee CH, Dogutan DK, Nocera DG. Hydrogen generation by hangman metalloporphyrins. *J. Am. Chem. Soc.* 2011; 133:8775–8777. [PubMed: 21557608]
31. Waibel R, et al. New derivatives of vitamin B12 show preferential targeting of tumors. *Cancer Res.* 2008; 68:2904–2911. [PubMed: 18413759]
32. Sambrook, J.; Russell, D. *Molecular cloning: A laboratory manual*. 3rd edn. Cold Spring Harbor Laboratory Press; 2001.
33. Wishart DS, Sykes BD. Chemical-Shifts as a Tool for Structure Determination. *Method. Enzymol.* 1994; 239:363–392.
34. Delaglio F, et al. NMRpipe - a Multidimensional Spectral Processing System Based on Unix Pipes. *J. Biomol. NMR.* 1995; 6:277–293. [PubMed: 8520220]
35. Vranken WF, et al. The CCPN data model for NMR spectroscopy: development of a software pipeline. *Proteins.* 2005; 59:687–696. [PubMed: 15815974]
36. Vevodova J, Graham RM, Raux E, Warren MJ, Wilson KS. Crystallization and preliminary structure analysis of CobE, an essential protein of cobalamin (vitamin B12) biosynthesis. *Acta Crystallogr. Sect. F Struct. Biol. Cryst. Commun.* 2005; 61:442–444.
37. Seyedarabi A, et al. Cloning, purification and preliminary crystallographic analysis of cobalamin methyltransferases from *Rhodobacter capsulatus*. *Acta Crystallogr. Sect. F Struct. Biol. Cryst. Commun.* 2010; 66:1652–1656.
38. Vagin A, Teplyakov A. Molecular replacement with MOLREP. *Acta Crystallogr. D.* 2010; 66:22–25. [PubMed: 20057045]
39. Brunger AT. Version 1.2 of the Crystallography and NMR system. *Nat Protoc.* 2007; 2:2728–2733. [PubMed: 18007608]
40. Cowtan K. The Buccaneer software for automated model building. 1. Tracing protein chains. *Acta Crystallogr. D.* 2006; 62:1002–1011. [PubMed: 16929101]
41. Murshudov GN, Vagin AA, Dodson EJ. Refinement of macromolecular structures by the maximum-likelihood method. *Acta Crystallogr. D.* 1997; 53:240–255. [PubMed: 15299926]
42. Emsley P, Lohkamp B, Scott WG, Cowtan K. Features and development of Coot. *Acta Crystallogr. D.* 2010; 66:486–501. [PubMed: 20383002]
43. Batty TGG, Kontogiannis L, Johnson O, Powell HR, Leslie AGW. iMOSFLM: a new graphical interface for diffraction-image processing with MOSFLM. *Acta Crystallogr. D.* 2011; 67:271–281. [PubMed: 21460445]
44. Blanc E, et al. Refinement of severely incomplete structures with maximum likelihood in BUSTER-TNT. *Acta Crystallogr. D.* 2004; 60:2210–2221. [PubMed: 15572774]
45. Winter G. xia2: an expert system for macromolecular crystallography data reduction. *J. Appl. Crystallogr.* 2010; 43:186–190.

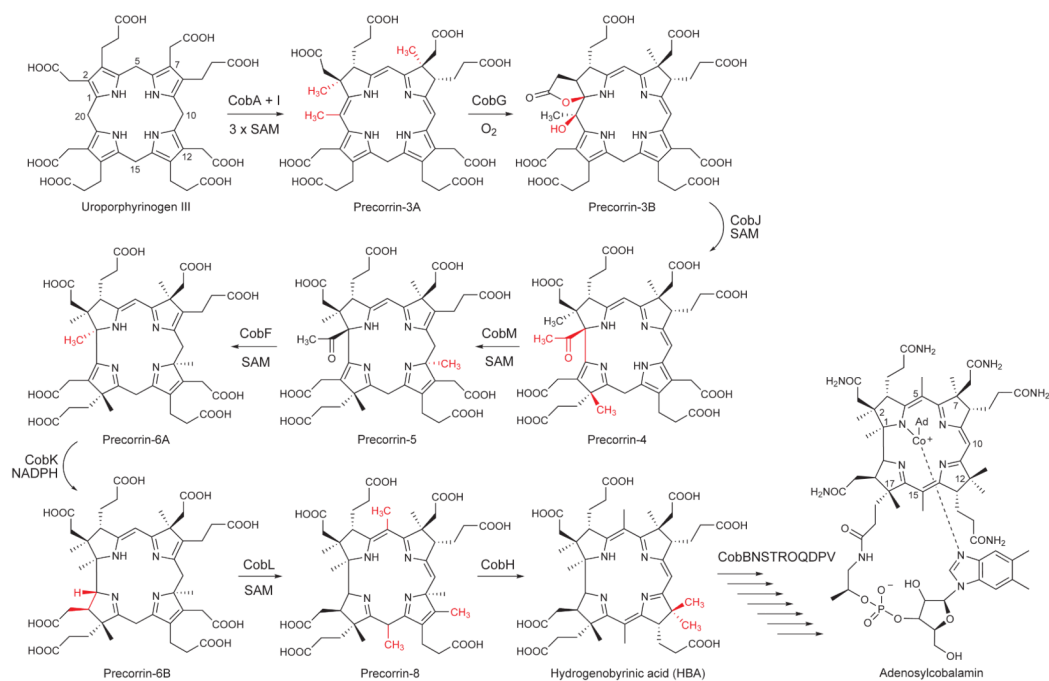


Figure 1. Transformation of uroporphyrinogen III into HBA and its position in the pathway in relation to adenosylcobalamin biosynthesis

There are 9 enzymes required for the synthesis of HBA from uroporphyrinogen III, six of which are SAM-dependent methyltransferases. The transformation of HBA into adenosylcobalamin requires a further 8 steps. In the adenosylcobalamin structure Ad stands for adenosine.

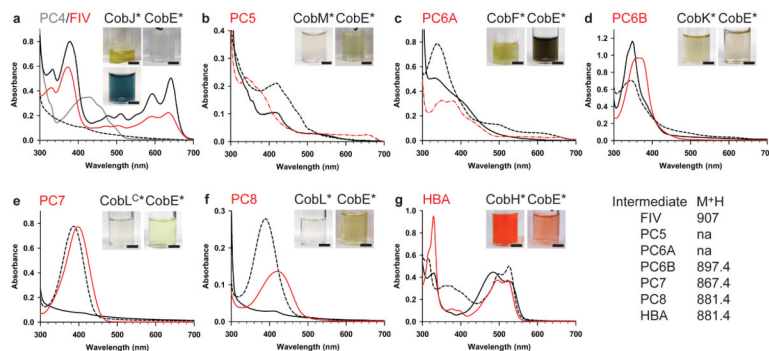


Figure 2. Spectral panoply of cobalamin intermediates isolated either via an enzyme-product complex, carrier-protein complex or by *in vitro* incubation

PC = precorrin and F = factor.

(a) Picture insets - Purified CobJ* isolates blue (aerobic) or yellow (anaerobic) from a strain overproducing CobA-I-G-J*. CobE* has no coloration when purified from a strain producing CobA-I-G-J-E*. Spectra are of anaerobically purified CobJ* (grey), aerobically purified CobJ* (black), intermediate released from aerobically purified CobJ* (red) and purified CobE* (dashed).

(b) Picture insets - Purified CobM* isolates pale yellow from a strain overproducing CobA-I-G-J-M*. CobE* has a stronger coloration when purified from a strain producing CobA-I-G-J-M-E*. Spectra are of purified CobM* (black), precorrin-5 produced by incubating precorrin-4 with CobM (red dashed) and purified CobE* (black dashed).

(c) Picture insets - Purified CobF* isolates yellow from a strain overproducing CobA-I-G-J-M-F*. CobE* has stronger coloration when purified from a strain producing CobA-I-G-J-M-F-E*. Spectra are of purified CobF* (black), precorrin-6A produced by incubating precorrin-4 with CobM and CobF (red dashed) and purified CobE* (black dashed).

(d) Picture insets - Purified CobK* isolates yellow from a strain overproducing CobA-I-G-J-M-F-K*. CobE* has less coloration when purified from a strain producing CobA-I-G-J-M-F-K-E*. Spectra are of purified CobK* (black), intermediate released from purified CobK* (red) and purified CobE* (black dashed).

(e) Picture insets - Purified CobL^C* isolates colorless from a strain overproducing CobA-I-G-J-M-F-K-L^C*. CobE* has yellow coloration when purified from a strain producing CobA-I-G-J-M-F-K-L^C-E*. Spectra are of CobL^C* (black), purified CobE* (black dashed) and the intermediate released from purified CobE* (red).

(f) Picture insets - Purified CobL* isolates colourless from strain overproducing CobA-I-G-J-M-F-K-L*. CobE* has yellow coloration when purified from strain producing CobA-I-G-J-M-F-K-L-E*. Spectra are of purified CobL* (black), purified CobE* (black dashed) and the intermediate released from purified CobE* (red).

(g) Picture insets - Purified CobH* isolates orange from a strain overproducing CobA-I-G-J-M-F-K-L-H*. CobE* is also orange when purified from a strain producing CobA-I-G-J-M-F-K-L-H-E*. Spectra are of purified CobH* (black), intermediate released from purified CobH* (red) and purified CobE* (black dashed).

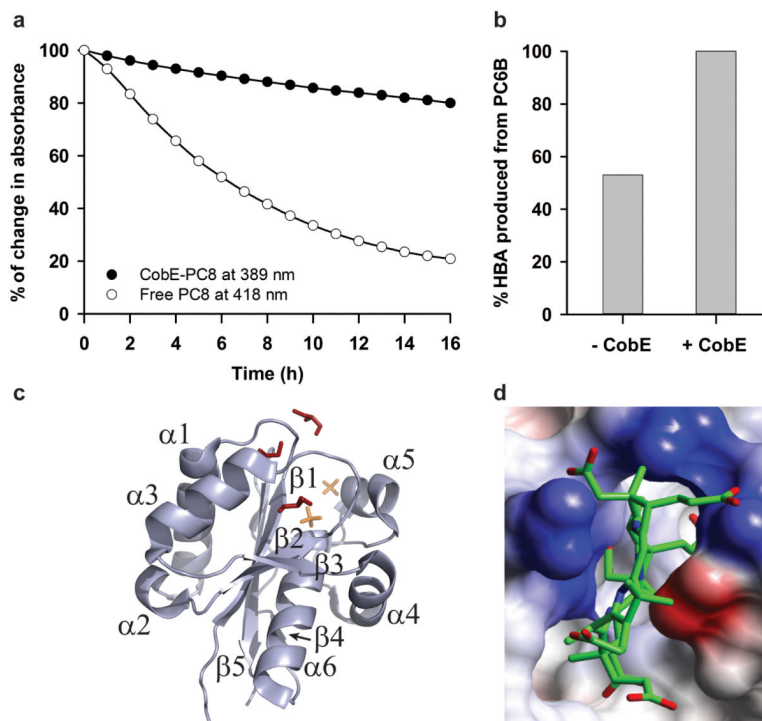


Figure 3. Role of CobE in the stabilization of precorrin-8 and the structure determination of the protein

- (a) Comparison of the stability of free and CobE-bound precorrin-8 (PC8) as monitored by loss of spectral features over time.
- (b) Comparison of the amount of HBA produced from precorrin-6B (PC6B) with CobL and CobH in the presence and absence of CobE.
- (c) Structure of CobE. The main crevice in the protein is formed between the β -sheet, α -helices α_5 and α_6 and the loops between β_1/α_1 and β_2/α_3 of CobE, which is where non-protein ligand molecules (glycerol and sulfate) are located.
- (d) Space-filling figure demonstrating the steric and electrostatic fit of HBA (fitted by PyMol) into the cavity in CobE. The CobH surface is colored according to charge with positive regions shown in blue and negative regions red. HBA is shown in stick representation.

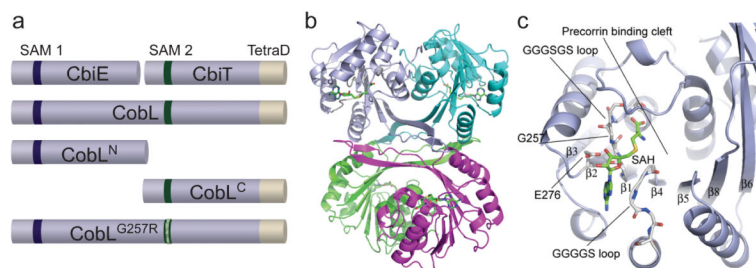


Figure 4. Structure analysis of CobL

(a) Cartoon demonstrating the dissection of CobL. The protein was dissected to give CobL^N and CobL^C, representing the N- and C-terminal regions of the protein. These regions align with the separate CbiE and CbiT proteins found in the anaerobic pathway (see Supplementary Figure 8). The figure also highlights one of the mutations that was introduced into CobL at position 257, within the second SAM binding site, to inactivate this region of the protein. The SAM binding regions and tetramerisation domain (TetraD) are also indicated.

(b) CobL^C structure. Cartoon of the tetrameric arrangement of four *R. capsulatus* CobL^C subunits with β -sheet and α -helices represented by arrows and helices respectively. Each polypeptide chain is a different color. The four SAH molecules, one in each of the four subunits, are drawn as sticks.

(c) The SAM binding site of the CobL^C subunit showing SAH bound at the C-terminal end of the Rossmann-like β/α fold. SAH binds between two glycine-rich loops that follow $\beta 1$ and $\beta 4$ respectively. The precorrin binding cleft is adjacent to the sulfur of SAH. Mutation of either E276 or G257 prevents SAM binding and destroys CobL^C C15 methylation and decarboxylation activity.

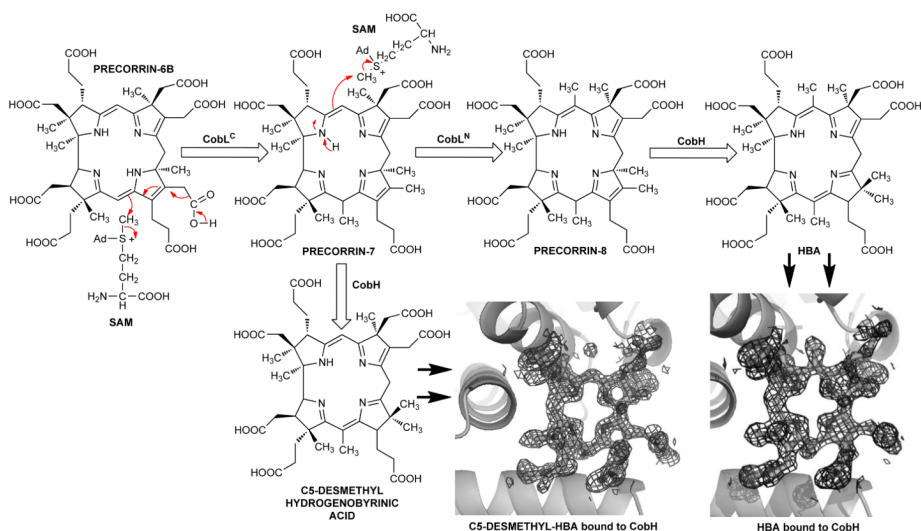


Figure 5. Transformation of precorrin-6B into HBA and C5-desmethyl-HBA

The acetic acid side chain attached to C12 of precorrin-6B is decarboxylated concomitantly with the methylation at C15 to generate precorrin-7 by the C-terminal region of CobL. Precorrin-7 is then methylated by the N-terminal region of CobL at C5 to give precorrin-8, which is converted into HBA by CobH. However, precorrin-7 can also act as an out-of-turn substrate for CobH. The structures of HBA and C5-desmethyl-HBA were determined by X-ray crystallography after binding them to CobH. The electron density for the C5 methyl group is clearly absent in the desmethyl compound. The map shown is the maximum likelihood/ σ_A weighted $2F_{\text{obs}} - F_{\text{calc}}$ density (contoured 1σ) in blue.